ResearchGate

See discussions, stats, and author profiles for this publication at:
https://www.researchgate.net/publication/224048603

Theoretical electronic structure of the alkali-dimer cation Rb-2(+)

ARTICLE *in* CHEMICAL PHYSICS · MAY 2003

Impact Factor: 1.65 · DOI: 10.1016/S0301-0104(03)00060-0

CITATIONS
15

READS
31

4 AUTHORS:

Alia Jraij
Lebanese University
16 PUBLICATIONS **78** CITATIONS
SEE PROFILE

Abdul-Rahman Allouche
Claude Bernard University Lyon 1
162 PUBLICATIONS **2,091** CITATIONS
SEE PROFILE

Mahmoud Korek
Beirut Arab University
103 PUBLICATIONS **714** CITATIONS
SEE PROFILE

M. Aubert-Frécon
Claude Bernard University Lyon 1
185 PUBLICATIONS **2,196** CITATIONS
SEE PROFILE

Available from: Alia Jraij
Retrieved on: 27 January 2016

Available online at www.sciencedirect.com
SCIENCE DIRECT®
Chemical Physics 290 (2003) 129–136
Chemical Physics
www.elsevier.com/locate/chemphys

Theoretical electronic structure of the alkali-dimer cation Rb_2^+

A. Jraij[a], A.R. Allouche[a], M. Korek[b], M. Aubert-Frécon[a,*]

[a] *Laboratoire de Spectrométrie Ionique et Moléculaire, CNRS et Université Lyon 1, Domaine Scientifique de La Doua, Bâtiment Alfred Kastler, F69622 Villeurbanne Cedex, France*
[b] *Beirut Arab University, P.O. Box 11–5020, Beirut, Lebanon*

Received 5 February 2003

Abstract

A theoretical study of the electronic structure of Rb_2^+ has been performed, including or not spin–orbit (SO) coupling. Potential energy curves for all the molecular states dissociating up to the limit $Rb^+ + Rb(7s\ ^2S_{1/2})$ (i.e., 26 states in the representation $^2\Lambda_{g,u}^{(+)}$ and 38 states in the representation $\Omega_{g,u}$) are displayed. Equilibrium distances, transition energies and depths for the wells predicted at short and large range of R are reported. The existence of some of the long-range wells are confirmed by a specific model. Extensive tables of energy values versus internuclear distances are available at the following address: http://lasim.univ-lyon1.fr/allouche/rb2plus.htm.
© 2003 Elsevier Science B.V. All rights reserved.

1. Introduction

Advances in the knowledge of ultralow temperature gases have induced recently a new interest in alkali-dimer cations. For instance, the electronic energies for the lowest states $^2\Sigma_g^+$ and $^2\Sigma_u^+$ of Na_2^+, in the whole range of internuclear distance R, have been used in studies of ultracold atom–ion collisions [1]. The knowledge of the long-range Coulombic and exchange interaction energies for the system $Na + Na^+$ was also involved in investigations of charge mobilities in an ultracold gas [2]. Furthermore, potential energy curves and transition dipole moments of alkali-dimer cations constitute basic data to study photodissociation processes [3–6]. They were used in wave packet dynamics simulations to establish that Rabi oscillations between dissociative molecular states are feasible in the Na_2^+ molecular ion [7,8]. Therefore, the usefulness of accurate data on the electronic structure of alkali homonuclear dimer cations has incited us to pursue our theoretical investigations in this scope.

While there exist theoretical data at disposal in the literature for the spectroscopy of the lighter homonuclear species Li_2^+, Na_2^+ and K_2^+ [9–21], corresponding data are more scarce for the heavier species Rb_2^+ [9–11,14]. These previous theoretical studies are restricted to the ground state [9,14] or to excited states dissociating up to the limit $Rb^+ + Rb(5p)$ [10,11]. More recently, diabatic potential energy curves obtained from an ab initio treatment were displayed for the $Rb^+ + Rb(nl)$

* Corresponding author. Tel.: +33-4-72-44-83-58; fax: +33-4-72-43-15-07.
E-mail address: frecon@lasim.univ-lyon1.fr (M. Aubert-Frécon).

0301-0104/03/$ - see front matter © 2003 Elsevier Science B.V. All rights reserved.
doi:10.1016/S0301-0104(03)00060-0

collisional system up to Rb(6p) [22]. We report here results of an ab initio study of all the molecular states in the two representations $^2\Lambda^{(+)}_{g,u}$ (neglecting SO effects) and $\Omega_{g,u}$ (including SO effects) dissociating into the limits up to $Rb^+ + Rb(7s\ ^2S_{1/2})$. Some long-range wells predicted at the ab initio level were seen to be reproducible with a specific model.

2. Summary of the theoretical approach

The Rb_2^+ ion is treated as a one-active electron system where the interaction between the external electron and each atomic ion is modelized through a non-empirical relativistic pseudopotential while polarization effects are taken into account through a core polarization potential. Spin–orbit (SO) effects are introduced via a semi-empirical spin–orbit pseudopotential W_{SO}. In the present work we use for Rb the same potential parameters (pseudo and core polarization), the same Gaussian basis set as well as the same SO pseudopotential as those used in our previous works on the electronic structure of RbCs [23,24]. For the rubidium atom, these previous calculations were seen to be very accurate for the five lowest states (errors lower than 0.6 cm^{-1}), somewhat less accurate for the higher states with the larger errors ($\sim$33 cm^{-1}) for the states 6nlm. In any case SO splittings were well reproduced for each state considered in the present work, as could be expected due to the fitting way by which the W_{SO} were determined. Molecular states $\Omega_{g,u}$ are obtained as the solutions of the total Hamiltonian approximated by $H_{tot} = W_{SO} + H_e$ and treated on the basis of the states $^2\Lambda_\Sigma$, solutions of H_e. Calculations have been performed using the CIPSO package [25]. The core–core interaction is evaluated as the ground state energy for the ion Rb_2^{2+} instead of the approximation $1/R$ which is not accurate enough for this species, at least for small values of the internuclear distance. This energy has been calculated using a pseudopotential from [26] and the basis set published for rubidium in our previous work on the electronic structure of KRb involving the ion KRb^{2+} [27].

3. Results

Calculations have been performed for 300 distances R from $4a_0$ to $130a_0$, for the 26 states $^2\Lambda^{(+)}_{g,u}$

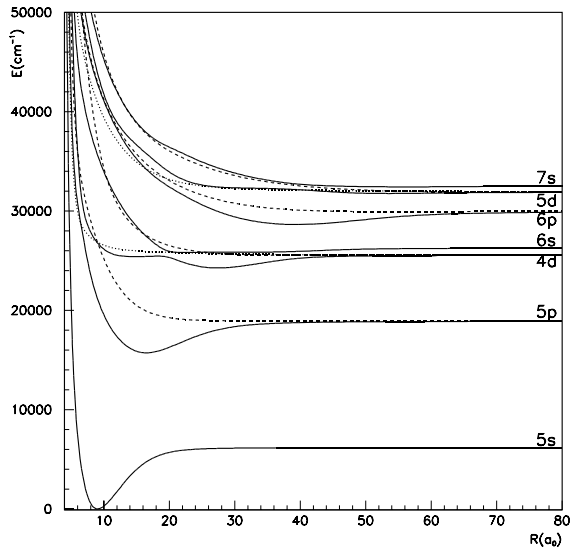

Fig. 1. Potential energy curves for the $^2\Lambda^{(+)}_g$ states of Rb_2^+. Full lines, $^2\Sigma^+_g$ states; dashed lines, $^2\Pi_g$ states; dotted lines, $^2\Delta_g$ states. The atomic state nl at dissociation is quoted.

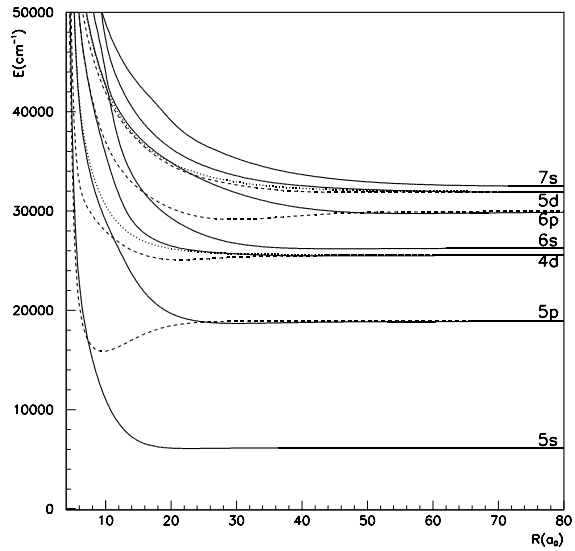

Fig. 2. Potential energy curves for the $^2\Lambda^{(+)}_u$ states of Rb_2^+. Full lines, $^2\Sigma^+_u$ states; dashed lines, $^2\Pi_u$ states; dotted lines, $^2\Delta_u$ states.

(neglecting SO effects) and for the 38 states $\Omega_{g,u}$ (including SO effects) dissociating to the limits up to $Rb^+ + Rb(7s\ ^2S_{1/2})$. Potential energy curves (PECs) for the $^2\Lambda^{(+)}_{g,u}$ states are drawn in Fig. 1 for the gerade states and in Fig. 2 for the ungerade ones. These PECs have rather complicated structures. Some states are found to be repulsive: the (1)–(2) $^2\Delta_{g,u}$; the (7) $^2\Sigma^+_u$ and the (1), (4) $^2\Pi_g$. Avoided crossings exist for various states of a given symmetry. An avoided crossing occurs at $R_{ac} \sim 20a_0$ between the states (3) and (4) $^2\Sigma^+_g$ with an energy difference between the two states ΔE_{ac} $\sim$600 cm^{-1}, in shorten notation (3)/(4) $^2\Sigma^+_g$ ($20a_0$, 600 cm^{-1}). Other avoided crossings can be quoted: the (5)/(6) $^2\Sigma^+_g$ ($10.8a_0$, 550 cm^{-1}), the (4)/(5) $^2\Sigma^+_u$ ($10.4a_0$, 780 cm^{-1}), the (6)/(7) $^2\Sigma^+_u$ ($9.4a_0$, 380 cm^{-1}) and the (2)/(3) $^2\Pi_g$ ($6.8a_0$, 810 cm^{-1}). Except for the (1) $^2\Sigma^+_g$ and the (1) $^2\Pi_u$ states for

Table 1
Spectroscopic constants (in cm^{-1}, R_e in a_0) for the $^2\Lambda^{(+)}_{g,u}$ states of Rb_2^+

State	T_e	R_e	ω_e	D_e
(1) $^2\Sigma^+_g$	0	9.06	45.96	6167
(1) $^2\Sigma^+_u$	6085	22.93	3.8	82
LR	6089	23.0	3.7	78
(2) $^2\Sigma^+_g$	15716	16.51	18.63	3188
(1) $^2\Pi_u$	15861	9.61	28.59	3043
Hump	18916	39.2	–	−12[a]
(2) $^2\Sigma^+_u$	18678	30.22	4.0	226
LR	18761	32.75	–	143
(2) $^2\Pi_u$	25067	21.46	7.8	455
(3) $^2\Sigma^+_g$	25398	14.97	7.8	124
Hump	25448	18.2	–	74[b]
	24262	27.36	9.8	1260
(3) $^2\Sigma^+_u$	25472	43.83	1.5	50
LR	25468	45.25	–	64
(2) $^2\Pi_g$	25509	44.74	–	13
LR	25429	35	–	93
(4) $^2\Sigma^+_g$	25821	22.2	9.2	448
(4) $^2\Sigma^+_u$	26192	45.93	1.7	76
LR	26233	49.5	–	68
(5) $^2\Sigma^+_g$	28628	39.43	6.3	1339
(3) $^2\Pi_u$	29142	29.67	7.8	824
(5) $^2\Sigma^+_u$	29741	56.57	2.2	225
LR	29804	64.5	–	130
(3) $^2\Pi_g$	29936	53.5	1.2	30
LR	29917	57	–	17
(6) $^2\Sigma^+_g$	31753	53.66	3.1	124
(7) $^2\Sigma^+_g$	32424	56.17	1.7	44

Long-range (LR) predictions are also quoted.
[a] Above the dissociation limit $Rb^+ + Rb(5p)$.
[b] Below the dissociation limit $Rb^+ + Rb(4d)$.

which the energy minima are located $\sim 9a_0$, the other bound states display wells at quite long range $R(\geqslant 16a_0)$. The state (3) $^2\Sigma_g^+$ has a double minimum structure. The inner well is small (124 cm^{-1}) while the outer one is 10 times larger (1260 cm^{-1}) the two being separated by a hump lying 74 cm^{-1} below the dissociation limit $Rb^+ + Rb(4d)$. The (1) $^2\Pi_u$ state displays a small hump at $R \sim 39a_0$ lying 12 cm^{-1} above the dissociation limit $Rb^+ + Rb(5p)$. The position of the wells as well as their depth (evaluated from the calculated atomic energy at the dissociation) are recorded in Table 1 together with the transition energies T_e evaluated from the bottom of the (1) $^2\Sigma_g^+$–PEC. The harmonic vibrational constant ω_e is also quoted in Table 1. For the ground state our value for the dissociation energy $D_e = 6167$ $cm^{-1} = 0.76$ eV is seen to be in very good agreement with both the experimental value for $D_0 = 0.73 \pm 0.06$ eV [28] and the accurate theoretical value $D_e = 0.76$ eV of [14] obtained from semi-empirical *l*-dependent pseudopotential calculations. An excellent agreement is also displayed with theoretical values of [14] for R_e and ω_e, we obtain 4.79 and 46 cm^{-1}, respectively, to be compared to 4.78 Å and 47 cm^{-1}.

The existence of some of the long-range wells can be predicted from a long-range model (LR), adding the Coulombic interaction to the exchange energy. It is the case for the series of $^2\Sigma_u^+$ states, for which the two contributions have opposite sign. The Coulombic interaction have been estimated in a perturbative way where the ion was assumed to interact at long range with the atom through its charge and its static dipole polarizability. Calculations were performed using simple one-electron wavefunctions, obtained for Rb via the process described in [29] involving only experimental atomic energies. To evaluate the exchange interaction energy, related to the indistinguishability of the dissociation limits $Rb^+ + Rb[nlm]$ and $Rb[nlm] + Rb^+$, we used the known asymptotic form of the surface integral method applied to the one–electron exchange case and recalled in [20], where once more the only parameters are the atomic energies $E(Rb[nl])$. Results derived from literature parameters are quoted in Table 1. For the $^2\Sigma_u^+$ states the long-range energy minima pointed out from ab initio calculations are also predicted from the long-range model with a reasonable accuracy. For the two $^2\Pi_g$ states bound at large R the LR model was also able to predict the existence of these small wells due to a competition between an attractive Coulombic interaction and a repulsive exchange energy.

As could be expected the situation is much more complex for the PECs corresponding to the various $\Omega_{g,u}$ states than it is for the $^2\Lambda_{g,u}$ ones, as seen from the Figs. 3–7 which present the PECs for the states $\Omega_g = 1/2$; $\Omega_g = 3/2$; $\Omega_u = 1/2$; $\Omega_u = 3/2$ and $\Omega_{g,u} = 5/2$, respectively. Some sharp avoided crossings ($\Delta E_{ac} < 100$ cm^{-1}) are evident for the symmetries $\Omega_{g,u} = 1/2$ and 3/2. They correspond in general to crossings between PECs of the $^2\Lambda_{g,u}$ states. The positions R_{ac} and the corresponding energy differences ΔE_{ac} are gathered in Table 2 together with the related crossing states. This results in the fact that for the symmetries $\Omega_{g,u} = 1/2$ and $\Omega_g = 3/2$, except for a few states, no unique main parent $^2\Lambda$ can be identified in the whole range of R. The only exceptions are the (1) $\Omega_g = 1/2$ with its main parent (1) $^2\Sigma_g^+$, the (7) $\Omega_g = 1/2$ [(5) $^2\Sigma_g^+$] and the (8) $\Omega_g = 1/2$ [(3) $^2\Pi_g$]. On the contrary, for

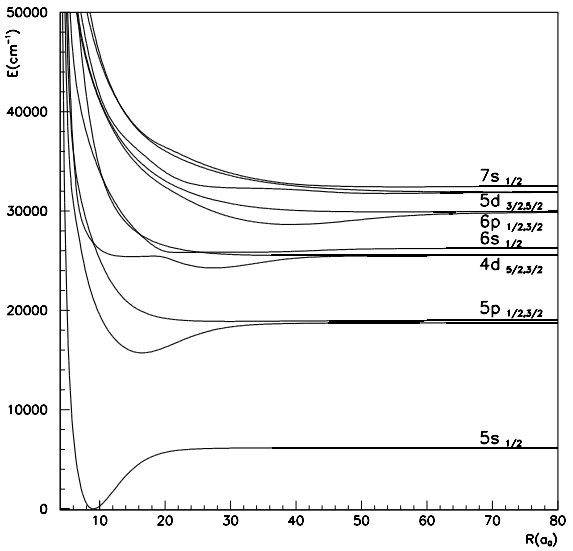

Fig. 3. Potential energy curves for the $\Omega_g = 1/2$ states of Rb_2^+. Atomic states $nl_{J1,J2}$ at dissociation are quoted, the component J1 being the lowest one.

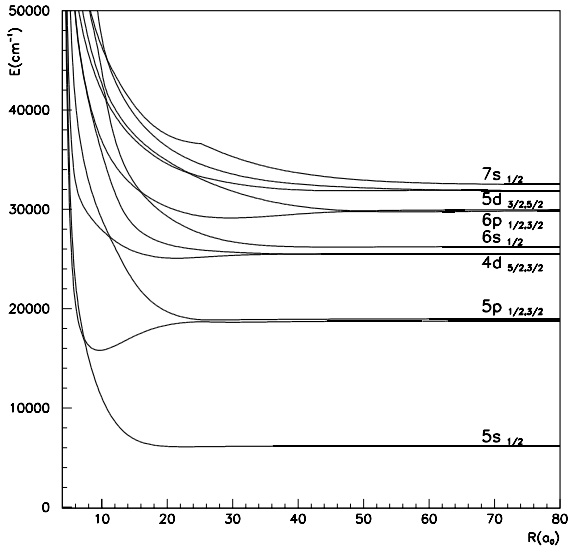

Fig. 4. Potential energy curves for the $\Omega_g = 3/2$ states of Rb_2^+.

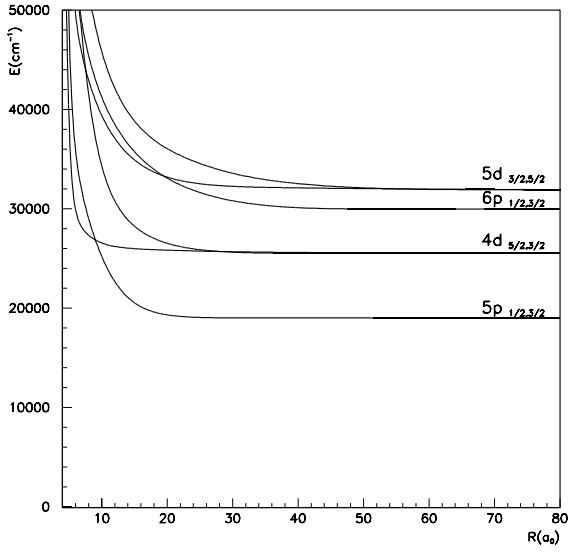

Fig. 5. Potential energy curves for the $\Omega_u = 1/2$ states of Rb_2^+.

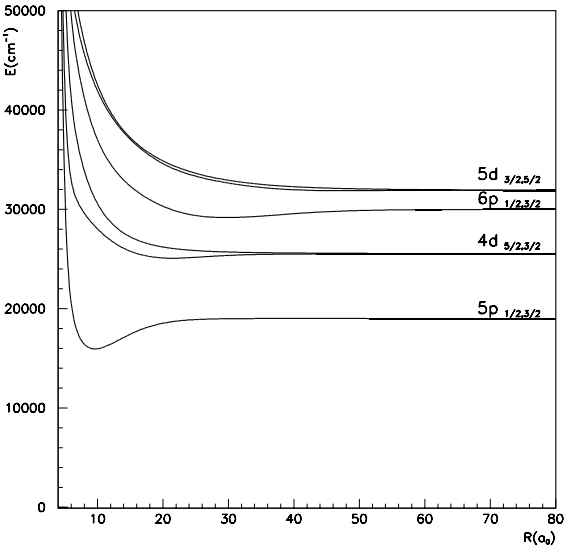

Fig. 6. Potential energy curves for the $\Omega_u = 3/2$ states of Rb_2^+.

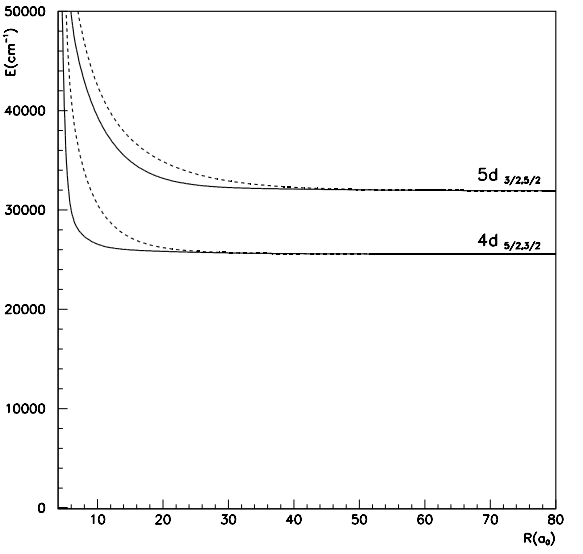

Fig. 7. Potential energy curves for the $\Omega_{g,u} = 5/2$ states of Rb_2^+. Full lines: g states, dashed lines: u states.

each state $\Omega_u = 3/2$ as well as for each state $\Omega_{g,u} = 5/2$ a main parent has been identified in the whole range of R. In any case, for most bound states $\Omega_{g,u}$ a main parent $^2\Lambda_{g,u}$ could be identified at the position of the energy minimum. The exceptions are the state (6) $1/2_g$ which has its minimum at the crossing between the PECs (4) $^2\Sigma_g^+/(2)\ ^2\Pi_g$, the state (3) $1/2_u$ which has its minimum not far from the crossing between the PECs (1) $^2\Pi_u/(2)\ ^2\Sigma_u^+$ and the state (5) $1/2_u$ which has its minimum at the crossing between the PECs (2) $^2\Pi_u/(3)\ ^2\Sigma_u^+$. This is illustrated in Fig. 8 where

Table 2
Some avoided crossings between Ω states

Symmetry	States n/n'	R_{ac}	ΔE_{ac}	Crossing $^2\Lambda$ states
$1/2_g$	3/4	6	16	(1) $^2\Pi_g/(3)$ $^2\Sigma_g^+$
		9	103	(3) $^2\Sigma_g^+/(1)$ $^2\Pi_g$
	4/5	20	611	–
	5/6	10.6	50	(4) $^2\Sigma_g^+/(2)$ $^2\Pi_g$
		16.2	13	(2) $^2\Pi_g/(4)$ $^2\Sigma_g^+$
		25.4	8	(4) $^2\Sigma_g^+/(2)$ $^2\Pi_g$
$3/2_g$	1/2	9	71	(1) $^2\Delta_g/(1)$ $^2\Pi_g$
	2/3	28	2	(1) $^2\Delta_g/(2)$ $^2\Pi_g$
	3/4	7.6	200	(2) $^2\Delta_g/(2)$ $^2\Pi_g$
	4/5	19.4	8	(2) $^2\Delta_g/(3)$ $^2\Pi_g$
$1/2_u$	1/2	7.4	225	(1) $^2\Pi_u/(1)$ $^2\Sigma_u^+$
	3/4	11.2	97	(2) $^2\Pi_u/(2)$ $^2\Sigma_u^+$
	5/6	7.4	150	(3) $^2\Pi_u/(3)$ $^2\Sigma_u^+$
	6/7	16	74	(3) $^2\Pi_u/(4)$ $^2\Sigma_u^+$
	7/8	49.5	66	(3) $^2\Pi_u/(5)$ $^2\Sigma_u^+$
$3/2_u$	5/6	15.4	161	

Position R_{ac} (in a_0) and corresponding energy difference ΔE_{ac} (in cm^{-1}). The related crossings of $^2\Lambda$ states are also quoted.

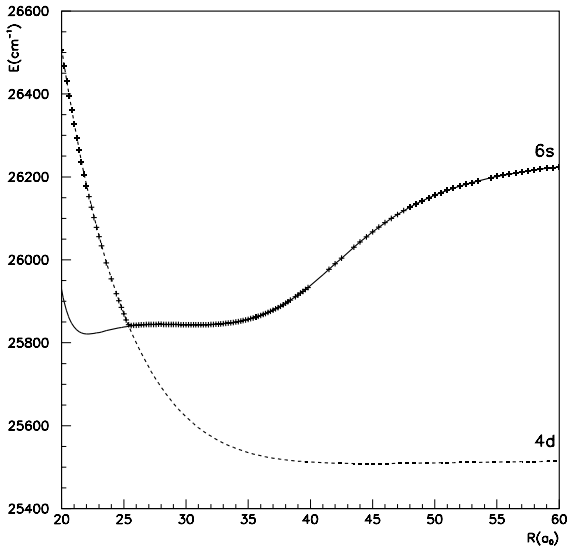

Fig. 8. Potential energy curves for the states (6) $1/2_g$ (points + + +), (2) $^2\Pi_g$ (dashed line) and (4) $^2\Sigma_g^+$ (full line).

are drawn the PECs for the two states (4) $^2\Sigma_g^+$ (correlating adiabatically to $Rb^+ + Rb(6s)$) and (2) $^2\Pi_g$ (correlating adiabatically to $Rb^+ + Rb$ (4d)) and the PEC for the state (6) $1/2_g$ (correlating adiabatically to $Rb^+ + Rb(6s\ ^2S_{1/2})$). Up to the crossing of the (4) $^2\Sigma_g^+$ and (2) $^2\Pi_g$ PECs ($\sim 25a_0$) the (6) $1/2_g$ and (2) $^2\Pi_g$ PECs are identical while for larger values of R the (6) $1/2_g$ PEC is identical to the (4) $^2\Sigma_g^+$ one. The position of the wells as well as the transition energies (evaluated from the bottom of the (1) $1/2_g$ ground state) are displayed in Table 3. The main parent when identified, at least at the bottom of the well, are also quoted in Table 3. From Table 3 the calculated splitting, evaluated at equilibrium distances, between the components 1/2 and 3/2 of the state (1) $^2\Pi_u$ dissociating into $Rb^+ + Rb$ (5p) is 142 cm^{-1}, a value which is compatible with the atomic SO splitting for Rb(5p), i.e., 237 cm^{-1}. The PECs for the (1) $^2\Pi_u$ state and its components 1/2 and 3/2 are displayed in Fig. 9

Table 3
Equilibrium internuclear distance R_e (in a_0) and transition energies T_e (in cm^{-1}, evaluated from the bottom of the ground state (1) $1/2_g$) for $\Omega_{g,u}$ states

Symmetry	State	T_e	R_e
$1/2_g$	(1) [(1) $^2\Sigma_g^+$]	0	9.06
	(2) [(2) $^2\Sigma_g^+$]	15714	16.52
	(3)	18879	29.92
	(4) [(3) $^2\Sigma_g^+$]	25399	14.92
	Hump	25448	18.2
	[(3) $^2\Sigma_g^+$]	24262	27.34
	(5) [(4) $^2\Sigma_g^+$]	25821	22.12
	Hump	25838	25.2
	[(2) $^2\Pi_g$]	25509	44.72
	(6)	25841	25.92
	(7) [(5) $^2\Sigma_g^+$]	28627	39.43
	(8) [(3) $^2\Pi_g$]	29913	53.38
$3/2_g$	(1) [(2) $^2\Pi_g$]	25509	44.62
	(4) [(3) $^2\Pi_g$]	29961	53.57
$1/2_u$	(1) [(1) $^2\Sigma_u^+$]	6085	22.92
	(2) [(1) $^2\Pi_u$]	15795	9.67
	(3)	18853	26.71
	(4) [(2) $^2\Pi_u$]	25067	21.48
	(5)	25488	39.4
	(6) [(4) $^2\Sigma_u^+$]	26192	45.93
	(7) [(3) $^2\Pi_u$]	29123	29.65
$3/2_u$	(1) [(1) $^2\Pi_u$]	15937	9.61
	(2) [(2) $^2\Pi_u$]	25067	21.51
	(4) [(3) $^2\Pi_u$]	29163	29.70

Main parents (identified at the bottom of $\Omega_{g,u}$ states) are quoted in parentheses.

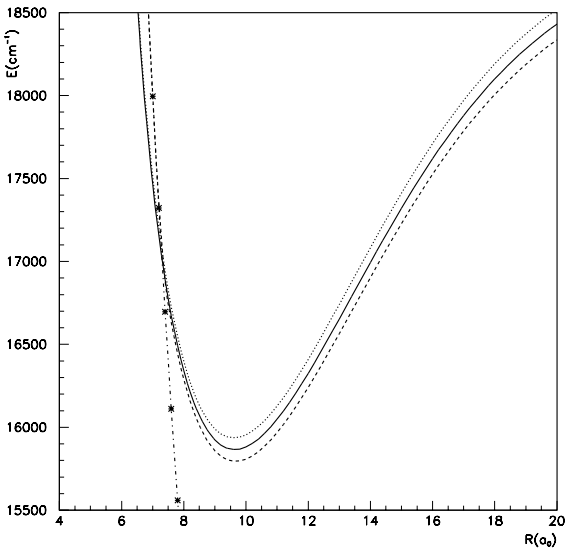

Fig. 9. Potential energy curves for the states (1) $^2\Pi_u$ (full line), (2) $1/2_u$ (dashed line), (1) $3/2_u$ (dotted line) and (1) $^2\Sigma_u^+$ (dashed-dotted line and points ✲).

showing the SO splittings at the bottom of the three curves. The crossing between the (1) $^2\Sigma_u^+$ and (1) $^2\Pi_u$ PECs ($\sim 7.3a_0$) is also visualized. Up to this crossing the (1) $3/2_u$ PEC is identical to the (1) $^2\Pi_u$ one, while the (2) $1/2_u$ PEC is identical to the (1) $^2\Sigma_u^+$ one. For the states (3) $^2\Pi_g$ and (3) $^2\Pi_u$ dissociating into $Rb^+ + Rb(6p)$, the molecular SO splittings are 48 and 40 cm^{-1}, respectively (atomic SO for $Rb(6p) = 77.5$ cm^{-1}). Note that at the precision of the present calculations we do not separate the components 1/2 and 3/2 of the (2) $^2\Pi_g$ and (2) $^2\Pi_u$ states dissociating into $Rb^+ + Rb(4d)$ (atomic SO for $Rb(4d) = 0.44$ cm^{-1}).

4. Conclusion

Ab initio calculations involving non-empirical pseudopotentials, core polarization potentials and semi-empirical spin–orbit pseudopotentials have been performed for the ground state as well as for 25 excited states of Rb_2^+ in a large range of internuclear distances. Various small wells at large values of R are predicted from these calculations, some of which are confirmed from a long-range specific model. As we hope that these data could be useful for further investigations we display extensive tables of energy values versus internuclear distance at the following address: http://lasim.univ-lyon1.fr/allouche/rb2plus.htm.

Acknowledgements

This work was supported by a joint funding from CNRS (France) and CNRS-L (Lebanon).

References

[1] R. Côté, A. Dalgarno, Phys. Rev. A 62 (2000) 012709.
[2] R. Côté, Phys. Rev. Lett. 85 (2000) 5316.
[3] S. Magnier, A. Toniolo, Chem. Phys. Lett. 338 (2001) 329.
[4] S. Magnier, M. Persico, N. Rahman, Laser Phys. 9 (1999) 403.
[5] S. Magnier, M. Persico, N. Rahman, Chem. Phys. Lett. 279 (1997) 361.
[6] S. Magnier, M. Persico, N. Rahman, Chem. Phys. Lett. 262 (1996) 747.
[7] G. Granucci, S. Magnier, M. Persico, J. Chem. Phys. 116 (2002) 1022.
[8] S. Magnier, M. Persico, N. Rahman, Phys. Rev. Lett. 83 (1999) 2159.
[9] L. Bellomonte, P. Cavaliere, G. Ferrante, J. Chem. Phys. 61 (1974) 3225.
[10] A. Valance, J. Chem. Phys. 69 (1978) 355.
[11] A.V. Nemuklin, N.F. Stepanov, Chem. Phys. Lett. 60 (1979) 421.
[12] I. Schmidt-Mink, W. Müller, W. Meyer, Chem. Phys. 92 (1985) 263.
[13] A. Bähring, I.V. Hertel, E. Meyer, W. Meyer, N. Spies, H. Schmidt, J. Phys. B 17 (1984) 2859.
[14] L. Von Szentpaly, P. Fuentealba, H. Preuss, H. Stoll, Chem. Phys. Lett. 93 (1982) 555.
[15] P. Fuentealba, H. Preuss, H. Stoll, L. Von Szentpaly, Chem. Phys. Lett. 89 (1982) 418.
[16] A. Henriet, F. Masnou-Seeuws, Chem. Phys. Lett. 101 (1983) 535.
[17] A. Henriet, J. Phys. B 18 (1985) 3085.
[18] E. Ilyabaev, U. Kaldor, J. Chem. Phys. 98 (1993) 7126.
[19] S. Magnier, F. Masnou-Seeuws, Mol. Phys. 89 (1996) 711.
[20] S. Magnier, S. Rousseau, A.R. Allouche, G. Hadinger, M. Aubert-Frécon, Chem. Phys. 246 (1999) 57.
[21] S. Magnier, M. Aubert-Frécon, JQSRT 78 (2003) 217.
[22] T. Romero, J. de Andrés, J. Sogas, J.M. Bocanegra, M. Alberti, J.M. Lucas, A. Aguilar, Chem. Phys. Lett. 292 (1998) 323.
[23] A.R. Allouche, M. Korek, K. Fakherddin, A. Chaalan, M. Dagher, F. Taher, M. Aubert-Frécon, J. Phys. B 33 (2000) 2307.

[24] H. Fahs, A.R. Allouche, M. Korek, M. Aubert-Frécon, J. Phys. B 35 (2002) 1501.
[25] C. Teichteil, M. Pelissier, F. Spiegelmann, Chem. Phys. 81 (1983) 273.
[26] P.J. Hay, W.R. Wadt, J. Chem. Phys. 82 (1985) 299.
[27] S. Rousseau, A.R. Allouche, M. Aubert-Frécon, J. Mol. Spectrosc. 203 (2000) 235.
[28] M. Shafi, L. Beckel, R. Engelke, J. Mol. Spectrosc. 42 (1972) 578.
[29] S.H. Patil, K.T. Tang, J. Chem. Phys. 106 (1997) 2298.